Japanese Journal of Applied Physics
Vol. 46, No. 9A, 2007, pp. 6022–6026

The Effectof Li-Ion-Doped Porous MgO Film on Operational Memory Margin of ac-Plasma Display Panel

Sung Il AHN, Heiju UCHIIKE[1], Seong Eui LEE[2], Kwangho KIM, and Sang Jik KWON*

Department of Electronic Engineering, Kyungwon University, Seongnam 461-701, Korea
[1]*Department of Information Display, Kyung Hee University, Seoul 130-701, Korea*
[2]*Department of Advanced Materials Engineering, Korea Polytechnic University, Shihung 429-793, Korea*

(Received February 12, 2007; revised June 9, 2007; accepted June 10, 2007; published online September 7, 2007)

An ac-type plasma display panel (ac-PDP) made with Li-ion-doped MgO film formed using a sol–gel precursor is characterized and compared with an ac-type PDP with an MgO film formed by e-beam evaporation. The operational memory margin of a test panel with a pure MgO film formed using the printing method is very high due to the porous surface of the films. For a test panel with Li-ion-doped MgO, the operational margin decreases as the dopant concentration increases. The secondary electron emission from a pure printed MgO film is highly unstable because of the severe surface charging due to the porosity of the MgO films. The surface charging decreases linearly as the dopant concentration increases. This secondary electron emission (SEE) result implies that a linear relationship exists between the memory margin of an ac-PDP and the charging phenomenon of the MgO surface after the SEE. [DOI: 10.1143/JJAP.46.6022]

KEYWORDS: ac-PDP, MgO, doping, secondary electron emission, porous

1. Introduction

The MgO film in an ac-type plasma display panel (ac-PDP) is bared in the gas discharging space so that the initial discharging voltage or operational voltage of the ac-PDP is affected by a secondary electron coefficient of MgO; moreover, the secondary electron coefficient depends on the crystalline structure and defect sites of the MgO films.[1–5)]

Reports on MgO materials indicate the possibility of obtaining a lower operational voltage condition by introducing impurities such as Li ion-making vacancies at anion sites and Al ion-making vacancies at cation sites in finally deposited MgO thin film.[6,7)] However, because the evaporation rates of the dopant and MgO are quite different, the vacancy levels produced by the thin film deposition are difficult to control. There is another difficulty in the characterization of MgO, particularly in the study of secondary electron emission (SEE) in relation to the discharge characteristics of an ac-PDP. The MgO layer, which is an insulator film whose surface is charged after electron emissions, has a considerable effect on the subsequent emissions of secondary electrons.[8–12)] MgO films formed using sol–gel precursors may have a more serious charging problem because they have a rougher surface and considerable more pores than MgO films formed by a vacuum technique. Theoretical research on SEE from the surface of porous MgO shows a marked increase in the degree of SEE due to the accumulation of charged particles near the pores.[13–15)] For an ac-PDP, two of the major factors in operation of ac-PDP are the wall charge, which is related to the operational voltage margin, and the initial firing voltage, which is related to the SEE yields from the MgO surface. Surprisingly, although the importance of charging in SEE studies is often noted, few reports have mentioned the relationship between the operational memory margin in an ac-PDP and the charging phenomenon on the MgO surface after the SEE. Moreover, while the relationship between impurities and operational memory margin is widely reported in the literature, the effect of the pores within the MgO film on the operational memory margin of an ac-PDP is rarely addressed.

In this study, we introduce condensed MgO films with a nano-sized pore structure from a sol–gel precursor. In addition, we introduce Li^+ ions as an impurity in the MgO films and control the doping level by varying the concentration of the sol–gel precursor. After fabricating a test panel of an ac-PDP with these materials, we examine the effect of the pores of the MgO film on the discharging properties of an ac-PDP with a Li^+ ion doped MgO film, and the relationship between the surface charging after the SEE and the operational memory margin.

2. Experimental Procedure

MgO precursor was prepared from a stabilized magnesium hydroxide sol that was derived from a starting material of magnesium methoxide. Firstly, a distilled acetylated carbitol solution with a stabilizer of naphthalene was prepared at 373 K for 10 min and then cooled down. At room temperature, the prepared solution was mixed with magnesium methoxide solution and then reacted with methanol solution containing distilled water. Finally, the solution was refluxed to remove methanol at 373 K for 10 min. The prepared sol was highly stable owing to the addition of naphthalene, even with a strong base such as lithium butoxide, which is a source of Li^+ ions. The prepared precursor sol was reacted with Li^+ source of lithium butoxide in mole ratios of 1000 to 3, 6, 12, and 24, and then dispersed into a screening solution of ethyl cellulose, acetylated carbitol, and terpineol.[16)]

Next, we prepared an e-beam-evaporated MgO layer of 200-nm-thick on a stainless steel plate as a reference for the SEE measurement and 500-nm-thick as a reference for the test panel. The prepared pastes were printed on a stainless steel plate and then calcined at 833 K for 1 h for the SEE experiments. After the calcination, we removed the oxidized Fe on the edge of the stainless steel to adjust the resistance. The thickness of the printed films was controlled in a range of 170–230 nm. The X-ray diffraction (XRD) spectra in Fig. 1 show that the printed MgO films were well crystallized with a strong (200) peak, which the intensity seems to be affected by the Li^+ ion content.

*Corresponding author.

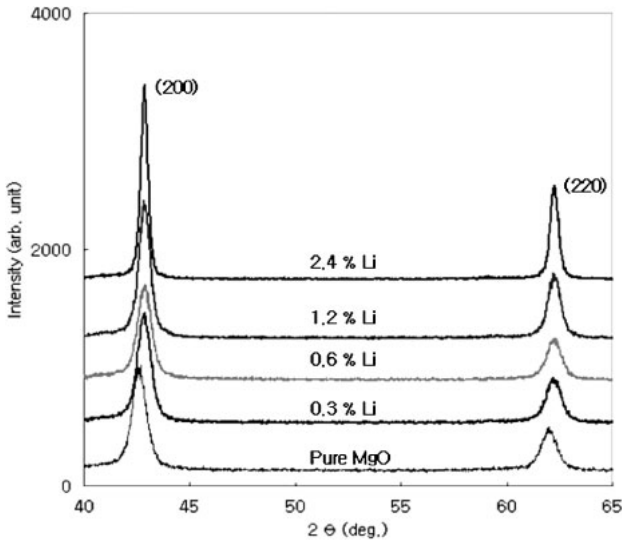

Fig. 1. XRD spectra of printed MgO films with different concentrations of Li^+ ions.

The experimental apparatus for measuring the secondary electrons consisted of an ion gun (SPECE-German), a measuring component, and a vacuum system.[17] The ion source was of the electron-bombardment ionization type, where the electrons emitted from a filament are accelerated in the discharge chamber. For the activation of samples, we attached a heater to the rear of the target; the temperature of the heater could be varied from room temperature to 673 K. The samples were activated under a high vacuum at 633 K for 6 h. We then injected Ne gas mixed with Xe gas 4% at 3×10^{-5} Torr into the ion-gun chamber. The acceleration voltage of the ion beam was fixed at 500 V, and the temperature was fixed at 583 K, where we observed stable SEE from the MgO film formed by e-beam evaporation.

To ensure relatively reproducible results, we designed the structure of the test panel of our ac-PDP to have saw-type electrodes, as shown in Fig. 2. Furthermore, to minimize fluctuations in the thicknesses of the dielectric layer and electrodes, the ac-type PDP cell was made of thin film ITO electrodes without the assistance electrodes, which are normally used in real ac-type PDP structures and a 2-μm-thick layer of SiO_2 was used as the dielectric layer formed by e-beam evaporation.

3. Results and Discussion

Figure 3 shows the surface morphology of a printed pure MgO film calcined at 833 K for 1 h. All the doped films had a morphology similar to that of the printed pure MgO. The morphology of the grain structure of the doped MgO films had a fine structure of homogeneous thin films with a well-controlled component ratio, irrespective of the dopant concentration in our experimental range. On the surface of the MgO there were many small pores, and a few large island-type defects, probably due to the fast hydrolysis reaction of the MgO precursor.

Figure 4 shows the firing voltages of test panels in which the MgO films have various concentrations of Li ions. All the doped samples have a lower firing voltage than the printed pure MgO film. In the case of the test panel with the highest level of doped MgO, after 100 min of aging, the firing voltage was similar to that of a panel with e-beam-evaporated MgO. In the first stage of aging, the panels with higher levels of doped MgO had a higher firing voltage than the panels with either a lower level of doped MgO or even pure MgO. The higher firing voltage is likely due to the surface contamination caused by the dopant ions on the surface.

Figure 5 shows the operational memory margin of the doped panels. We can observe a clear connection between the doping and the decreased operational memory margin as the aging time progresses; also, we can observe a linear relationship between the dopant concentration and the operational memory margin after 50 min of aging. The panel with the pure printed MgO, for instance, has a higher operational memory margin than any other panels with a different type of MgO. This phenomenon can be explained by the porous surface structure of the printed MgO (which resembles the characteristics of the SEE graphs in Fig. 7).

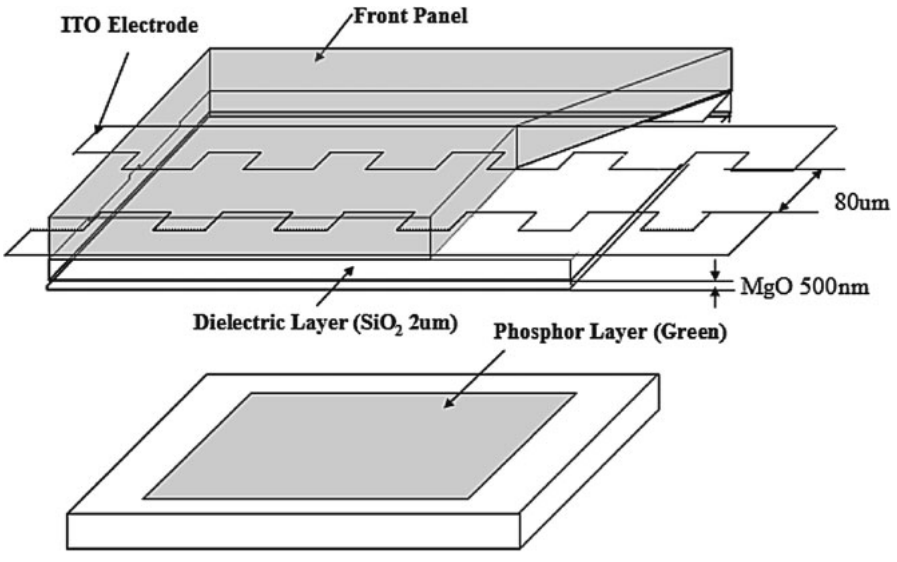

Fig. 2. Structure of ac-PDP used in this experiment. (The test panel has 48 cells and a 100 μm gap between the front and rear panels.)

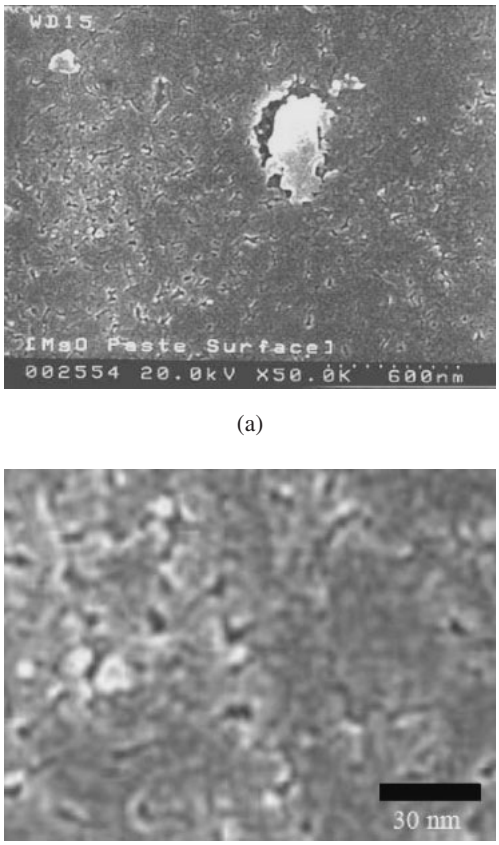

(a)

(b)

Fig. 3. SEM image of MgO film fired at 833 K for 1 h: (a) surface and (b) magnified surface of (a).

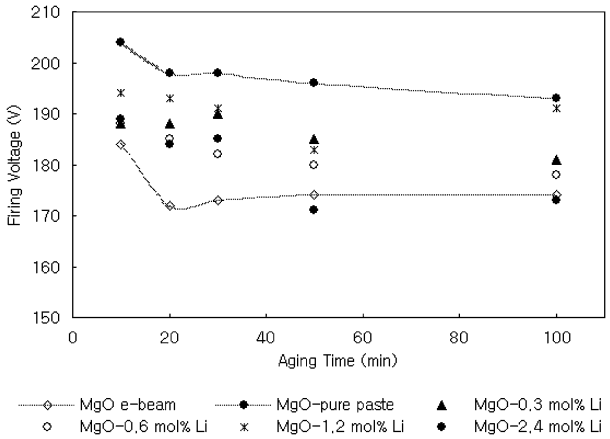

Fig. 4. Initial firing voltages of test panels with various MgO films versus aging time. (Every panel was activated at 833 K for 5 h under high vacuum.)

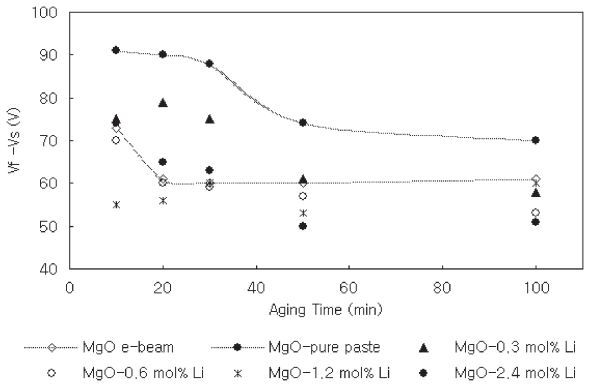

(a)

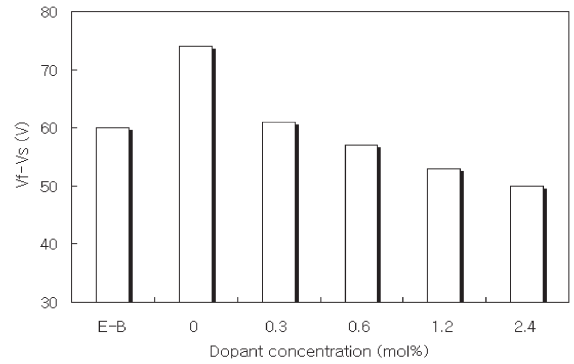

(b)

Fig. 5. Operational memory margin of ac-PDP with various MgO films. (E-B is the MgO film formed by e-beam evaporation): (a) $V_f - V_s$ versus aging time and (b) $V_f - V_s$ versus dopant concentration after 50 min of aging.

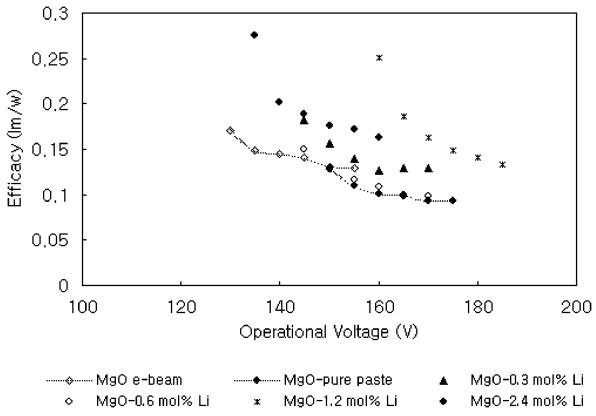

Fig. 6. Luminous efficacy of test panels with various MgO films versus operational voltages after 50 min of aging.

Many charged particles appear during the discharging process and these particles may stay and survive longer in the surface pores. If the charged particles stay longer in the pores during the operation of an ac-PDP, the effect may be considerable, that is, an increase in the wall charge may lead to a wider operational memory margin. Supposing that the surface of doped MgO films has a similar porosity to that of printed pure MgO films, the doping of Li ion in MgO appears to inhibit the accumulation of charged particles on the surface of MgO. The change in the operational memory margin indicates a decrease in the number of charged particles on the surface of the doped MgO film. This result is in good agreement with the result of a previous report on Li-ion-doped MgO, which showed that structural defects are related to changes in conductivity.[18)]

The result of luminous efficiency in Fig. 6 shows that the panels with doped MgO have higher luminous efficiencies than the e-beam-evaporated MgO film, irrespective of the dopant concentration. Interestingly, all the panels with the printed MgO, except for the panel with the printed pure MgO, show a considerably lower current consumption

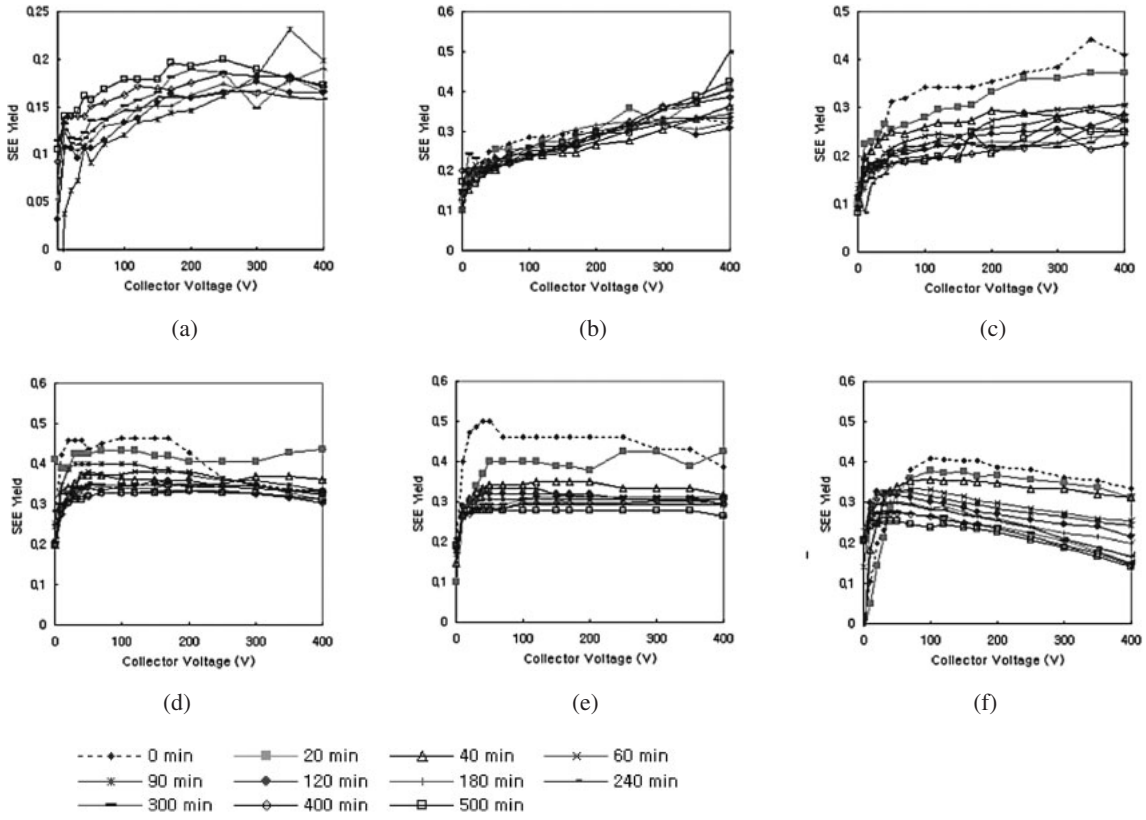

Fig. 7. Surface charging trend dependent on measuring time of SEE. (In the case of the printed pure MgO film, the SEE data measured at 0, 20 and 40 min are omitted owing to the serious fluctuation.): (a) printed pure MgO, (b) printed MgO with 0.3 mol % Li^+, (c) printed MgO with 0.6 mol % Li^+, (d) printed MgO with 1.2 mol % Li^+, (e) printed MgO with 2.4 mol % Li^+, and (f) MgO formed by e-beam evaporation.

during the discharge than the panel with the e-beam-evaporated MgO.

The SEE yield for every sample was measured from the first few minutes to 500 min and plotted versus collector voltage in Fig. 7. We observed two important phenomena in the SEE results. The first is the fact that the doped MgO has a higher SEE yield than the printed pure MgO and the other is that the emission of the secondary electron is stabilized as the dopant concentration is increased. It is very hard to compare the SEE yields directly without considering the well-known factors, such as the field emission and the abnormal emission near the pores.[8–10] Between the printed samples, however, we can compare the relative SEE yields supposing that they have a similarity in pore structure and density. The high SEE yield from the Li-ion-doped MgO compared with the printed pure MgO film in Fig. 6 can be explained by two major factors: firstly, the creation of a defective band that enables the emission of secondary electrons from the Xe gas ions;[19] and, secondly, the enhanced crystallization of MgO by the addition of Li^+ ions.[20]

An experimental condition for measuring the SEE is satisfied when stable SEE can be observed from the e-beam-evaporated MgO. The heating of substrates seems to effectively remove the surface charging of the evaporated MgO film; however, it does not completely remove the surface charging of porous MgO films. Reports on SEE from MgO layers having pores suggest that the growth of strong electric fields throughout the pores produces higher SEE yields than those of bulk MgO materials.[14,15] The trend of the saturation of SEE, which is related to the amount of surface charging, in Fig. 7 shows a proportional relationship to the dopant concentration. From this result, we also consider a proportional relationship between the amount of surface charging occurring during the SEE measurement and the operational memory margin of an ac-PDP.

4. Conclusions

Condensed and Li-ion-doped MgO films with a nano sized pore structure were introduced and characterized in an ac-PDP structure. With respect to the discharge characteristics, the printed pure MgO film shows two phenomena: they have the highest initial firing voltage due to a low SEE property and the widest operational voltage margin owing to the porous surface structure. The Li-ion-doped MgO reduces the initial firing voltage of an ac-PDP; it also reduces the operational memory margin of an ac-PDP, probably due to the increased conductivity of the MgO film. The SEE results showed a linear relationship between the amount of surface charging occurring during the SEE measurement and the operational memory margin of an ac-PDP.

1) E. Choi, H. Oh, Y. Kim, J. Ko, J. Lim, J. Kim, D. Kim, G. Cho, and S. Kang: Jpn. J. Appl. Phys. **37** (1998) 7015.
2) Y. Kim, R. Kim, H. J. Kim, H. Jeon, and J. W. Park: Mater. Res. Soc. Symp. Proc. **621** (2000) Q5.6.1.
3) J. S. Oh and E. H. Choi: Jpn. J. Appl. Phys. **43** (2004) 1154.
4) Y. Murakami, H. Matsuzaki, H. Murakami, and N. Ikuta: Jpn. J. Appl.

Phys. **40** (2001) 3382.
5) T. Tsujita, T. Nagatomi, Y. Takai, Y. Morita, M. Nishitani, M. Kitagawa, and T. Uenoyama: Jpn. J. Appl. Phys. **43** (2004) 753.
6) L. A. Kappers, R. L. Kroes, and E. B. Hensley: Phys. Rev. B **1** (1970) 4151.
7) K. H. Park and Y. S. Kim: IMID/IDMC'06 Dig. 2006, p. 375.
8) J. J. Scholtz, R. W. A. Schmite, B. H. W. Hendriks, and S. T. de Zwart: Appl. Surf. Sci. **111** (1997) 259.
9) Y. Mizuhara, J. Kato, T. Nagatomi, Y. Takai, and M. Inoue: J. Appl. Phys. **92** (2002) 6128.
10) K. Ohya, T. Itotani, and J. Kawata: Jpn. J. Appl. Phys. **33** (1994) 1153.
11) J. Cazaux, K. H. Kim, O. Jbara, and G. Salace: J. Appl. Phys. **70** (1991) 960.
12) T. Kamiya, M. Cholewa, A. Saint, S. Prawer, G. J. F. Legge, J. E. Butler, and D. J. Vestyck, Jr.: Appl. Phys. Lett. **71** (1997) 1875.
13) K. I. Grais and A. M. Bastawros: Jpn. J. Appl. Phys. **19** (1980) 2089.
14) H. Jacobs, J. Freely, and F. A. Brandt: Phys. Rev. **88** (1952) 492.
15) J. M. Millet and J. J. Lafon: Phys. Rev. A **52** (1995) 433.
16) S. I. Ahn: U.S. Patent 6335393 (2002).
17) K. Yoshida, H. Uchiike, and H. Sawa: IEICE Trans. Electron. **E82-C** (1999) 1798.
18) I. Balint and K. Aika: Appl. Surf. Sci. **173** (2001) 296.
19) Y. Motoyama, Y. Hirano, K. Ishii, Y. Murakami, and F. Sato: J. Appl. Phys. **95** (2004) 8419.
20) H. Aritani, H. Yamada, T. Nishio, T. Shiono, S. Imamura, M. Kuno, S. Hasegawa, T. Tanaka, and S. Yoshida: J. Phys. Chem. B **104** (2000) 10133.